

1 **Real-time aerosol chloride deposition measuring device using a conductivity sensor**

2

3 Ngoc Duc Pham^{*1,2} (Corresponding Author)

4 ¹RACE (Research into Artifacts, Center for Engineering), The University of Tokyo,5-1-5 Kashiwanoha,
5 Kashiwa, Chiba 277-8568, JAPAN

6 Tel: +81-4-7136-4240 Fax: +81-4-7136-4242 E-mail: duc@race.u-tokyo.ac.jp

Shinji Okazaki³ E-mail: okazaki-shinji-yp@ynu.ac.jp

Yukihisa Kuriyama¹ E-mail: kuriyama@race.u-tokyo.ac.jp

Naoya Kasai³ E-mail: kasai-naoya-pf@ynu.ac.jp

Katsuyuki Suzuki¹ E-mail: katsu@race.u-tokyo.ac.jp

7 Affiliations

8 ¹RACE (Research into Artifacts, Center for Engineering), The University of Tokyo,5-1-5 Kashiwanoha,
9 Kashiwa, Chiba 277-8568, JAPAN

10 ²Faculty of Road & Bridge Engineering, The University of Danang, University of Science and
11 Technology, No.54 Nguyen Luong Bang Str., Lien Chieu Dist., Da Nang City, VIETNAM.

12 ³Yokohama National University, 79-5 Tokiwadai, Hodogaya-ku, Yokohama 240-8501, JAPAN.

13 **Title**

14 Real-time aerosol chloride deposition measuring device using a conductivity sensor

15

16 **Abstract.**

17 This study proposes a new monitoring method to measure real-time aerosol chloride deposition. The
18 concept of a water candle device is introduced, and the device is manufactured. By continuously generating
19 a thin water film in combination with a conductivity sensor, the device is capable of measuring aerosol
20 chloride deposition in all directions and has a compact design. The water candle device was fully tested in
21 the laboratory and applied to monitor on a bridge. For the laboratory tests, the transport of aerosol in an
22 area near the seashore was simulated to evaluate the accuracy and responsiveness of the device according
23 to the variable wind speed and source salt concentration. For monitoring in the field, the device was
24 implemented at the Thuan Phuoc Bridge, Vietnam, for seven days with a short recording frequency of a
25 few hours. A set of wet candle devices were placed next to the water candle device to compare the results
26 of the two methods. The results of the laboratory test and field monitoring demonstrated a high accuracy
27 and responsiveness of the water candle device to variations in the wind speed and salt concentration of the
28 source. Further, there were only very small differences between the results from the wet and water candle
29 devices.

30

31 **Keywords.**

32 Real-time aerosol chloride deposition measurement, wet candle method, bridge, aerosol transport,
33 conductivity sensor

34 **1. Introduction**

35 Corrosion is a significant issue for structures, especially in coastal areas. Chloride ions are one of the
36 main factors that cause corrosion (Ahmad, 2006; Revie et al., 2008; Corvo et al., 1995; Silman et al., 1972).
37 High amounts of chloride accumulated on the surface vastly accelerate the corrosion of metal or concrete
38 structures (Corvo et al., 1995; Britton et al., 1976; Foley et al., 1970). Therefore, chloride deposition
39 monitoring is crucial for the proper maintenance of structures. Chloride deposition monitoring is mainly
40 used for the measurement of aerosol chloride deposited on a certain area. Aerosol chloride is generated
41 from diverse locations such as forest, urban area, marine and coastal area. In forest, agricultural areas,
42 aerosol chloride contains in fine particles in biomass burning plumes (Pratt et al., 2011). In industrialized
43 urban areas, metal chlorides contribute as much as 73% to the fine particles emitted in industrial smoke
44 (Moffet et al., 2008a). In marine and coastal area, aerosol chloride is contained in small particles generated
45 from the ocean (Meira et al., 2008; Meira et al., 2006; Hossain et al., 2009; Fitzgerald et al., 1991; Spiel et
46 al., 1996). These particles are transported onto land by the wind and deposited onto structures (Hossain et
47 al., 2009; Gustafsson et al., 2000; Meira et al., 2007; Lee et al., 2006; Delalieux et al., 2006; Meira et al.,
48 2017; Feilu et al., 1999).

49 There are many methods for monitoring chloride deposition, such as the dry gauze (JIS Z 2382, 1998),
50 DOKEN (N. Kazuhiro and D. Yoshiki 1993), K3 (Lee and Moon 2006), and wet candle (ISO 9225, 2012)
51 methods. The dry gauze, K3, and DOKEN methods utilise a dry gauze to cover a flat surface or a stainless
52 plate to capture the aerosol chloride. The dry gauze method requires a large area of 2 m×2 m and is therefore
53 difficult to install on bridges. The DOKEN and K3 methods have smaller consuming areas of ~0.5 m×0.4
54 m but have dry gauze or stainless plates installed in a box with one opening. Hence, these methods can
55 collect aerosols mainly coming from one direction perpendicular to the opening. The wet candle device,
56 with a consuming area of 0.5 m×0.5 m, uses a gauze wrapped around a pipe, enabling the collection of
57 aerosols from all directions.

58 The wet candle method has been applied to aerosol chloride monitoring (Meira et al., 2006; Meira et al.,
59 2017; Anwar Hossain, Easa and Lachemi, 2009). Studies have been conducted by long-term monitoring
60 with monthly or longer sampling frequencies (Lee and Moon, 2006; Meira et al., 2006; Anwar Hossain,
61 Easa and Lachemi, 2009; Morcillo et al., 2000). However, chloride deposition significantly increases in
62 unfavourable weather events, such as typhoons, atmospheric depressions, or even strong winds (Morcillo
63 et al., 2000; Pham et al., 2019; Meira et al., 2007), which usually last for a short time of a few days.
64 Therefore, long sampling frequency data cannot be used to determine the rapid accumulation of aerosol
65 chloride.

66 The shorter the sampling frequency, the better the chloride deposition evaluation; hence, appropriate
67 maintenance of a structure may be performed. In a recent study (Pham et al. 2019), we carried out the long-
68 term measurement of aerosol chloride in Da Nang city, Vietnam, with a weekly sampling frequency using
69 the wet candle method. The monitored data contained the details of the rapid accumulation of aerosol
70 chloride in a short period of an unfavourable weather event. However, typhoons and depressions can last a
71 week or even a day, and therefore daily or shorter sampling frequency monitoring is required to determine
72 the mechanisms responsible for aerosol chloride accumulation during these weather events. To the best of
73 our knowledge, no study exists on the real-time monitoring of aerosol chloride deposition; hence, it is of
74 great interest to obtain real-time monitoring of chloride deposition.

75 Measurements using wet candle devices require many operation steps. In the preparation step, each part
76 of the wet candle device is washed to remove any chloride, and the device is carefully covered to avoid
77 contaminants when transported to the site. After the monitoring period, the gauze is carefully collected and
78 placed in distilled water for 24 h before extraction into a small cell for chloride analysis by the adsorption
79 spectroscopy method. The whole measurement process and chloride content analysis requires expert
80 personnel to avoid contamination and to obtain accurate results. Conversely, real-time monitoring requires
81 less operation steps during monitoring and can be conducted by unskilled personnel.

82 This study proposes a real-time aerosol chloride measuring device. The device collects aerosol chloride,
83 similar to the wet candle device, by a thin water film instead of wet gauze. A conductivity sensor is installed
84 in the device to measure the aerosol chloride in real-time. The device is named a “water candle”, analogous
85 to the wet candle device. The accuracy and responsiveness of the device was tested in a laboratory. In
86 addition, it was successfully implemented in the field in Da Nang city, Vietnam, and the measured results
87 showed good agreement with those of the wet candle device.

88 **2. Methods**

89 **2.1 Device concept**

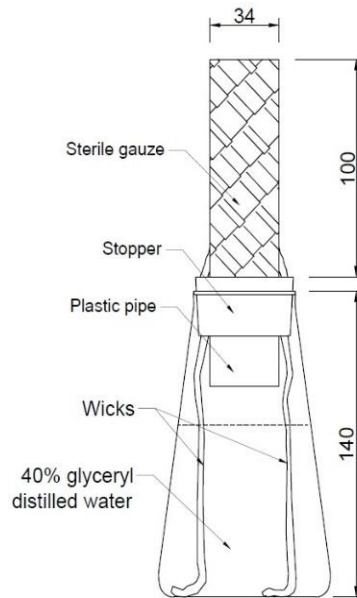


Figure 1 Wet candle device (Pham et al.,2019)

90 The wet candle method has been employed to measure aerosol chloride (Meira et al., 2006; Meira et al.,
91 2017; Anwar Hossain, Easa and Lachemi, 2009). **Fig. 1** shows the assembly of a wet candle device, which
92 consists of two parts. The upper part includes a plastic pipe covered by gauze to capture the aerosol chloride,
93 and the lower part contains a reservoir of glyceryl-distilled water to maintain the wet condition of the gauze.
94 Because the gauze is kept wet and wrapped around the pipe, it can capture aerosols blown from all directions.
95 After the designated monitoring period, the gauze is placed into a new 600 mL beaker. The glyceryl-
96 distilled water is poured into the same beaker. After rinsing the pipe, flask, and stopper with distilled water,
97 and adding it to the beaker, the contents are adjusted to 500 mL and kept for at least 24 h before the chloride
98 content analysis. The gauze is then wrung to drain water into the beaker. The remaining content is extracted
99 to a small cell for the chloride content analysis by the absorption spectroscopy or chromatography methods.

100 As described above, the treatment and analysis process for a wet candle sample includes many
101 operation steps, and the cumulative errors from each step can result in large errors of the final analysis
102 result. Therefore, the measurement and chloride content analysis of a wet candle sample requires expertise
103 to obtain accurate results.

104 This study proposes a new device that replaces the gauze with a thin water film to capture and dissolve
105 aerosols. In this way, the device is applicable to real-time chloride deposition monitoring without any
106 further human intervention after the preparation is completed. This therefore reduces analysis errors and
107 treatment steps, compared with conventional analysis methods. As shown in **Fig. 2**, water is circulated
108 through the device. To perform the chloride content analysis, a conductivity sensor is immersed into the

109 reservoir to record the changes in the conductivity caused by dissolved aerosol chloride ions. Although this
110 concept consumes electricity to maintain the water film, it can eliminate almost all of the disadvantages of
111 the wet candle method.

112 **Figure 2** shows the assembly of the new device consisting of a cylinder glass pipe; beaker containing
113 distilled water and 40% glyceryl; 12 W pump to circulate the solution from the beaker to the glass pipe,
114 and back to the beaker to form a thin water film around the surface of the pipe; conductivity sensor to
115 monitor the change in the conductivity of solution; and stopper to support and fix the sensor and pipe.
116 Moreover, the glass pipe is connected to the pump through a small plastic tube. A rubber plug is attached
117 to the top of the glass pipe to modify the run-out water to produce an equal-distribution of the water film
118 (the so-called floating plug). The surface of the glass pipe was brushed by sand-paper, No. 80, to maintain
119 an equal distribution of the water film. The thickness of the water film is minimal due to the dispersal by
120 strong wind. The thickness can be adjusted by the pumping speed of the pump via a valve. If the out-put
121 rate is high, the thickness of water film becomes too large, causing water film easily blown out by strong
122 wind. On the contrary, if the out-put rate is low, the run-out of water splits into small individual water
123 streams and unable to keep uniform water film overall the surface of the glass pipe. Preliminary
124 measurement showed that the width of water film was appropriate at 1 – 1.5 mm. As a result, the water out-
125 put rate was chosen at 25 mL s⁻¹.

126 Before starting the new device, all components were washed with distilled water, and the pump was fixed
127 to the bottom of beaker. The solution in water candle device was circulated through the pump until there is
128 no change of conductivity (about 2 hours). This is to ensure there are no contaminants effecting the
129 conductivity. A volume of 400 mL of 40% glyceryl distilled water is placed in beaker, and the connecting
130 pipe is attached to the pump by a plastic tube and fixed to the stopper. The stopper is adjusted to fix it to
131 the beaker wall. The conductivity sensor is attached to and carried by the stopper and merged into the

132 solution. The accuracy and responsiveness of the device were tested in the laboratory and implemented in
133 the field at Thuan Phuoc Bridge, Da Nang city, for seven days.

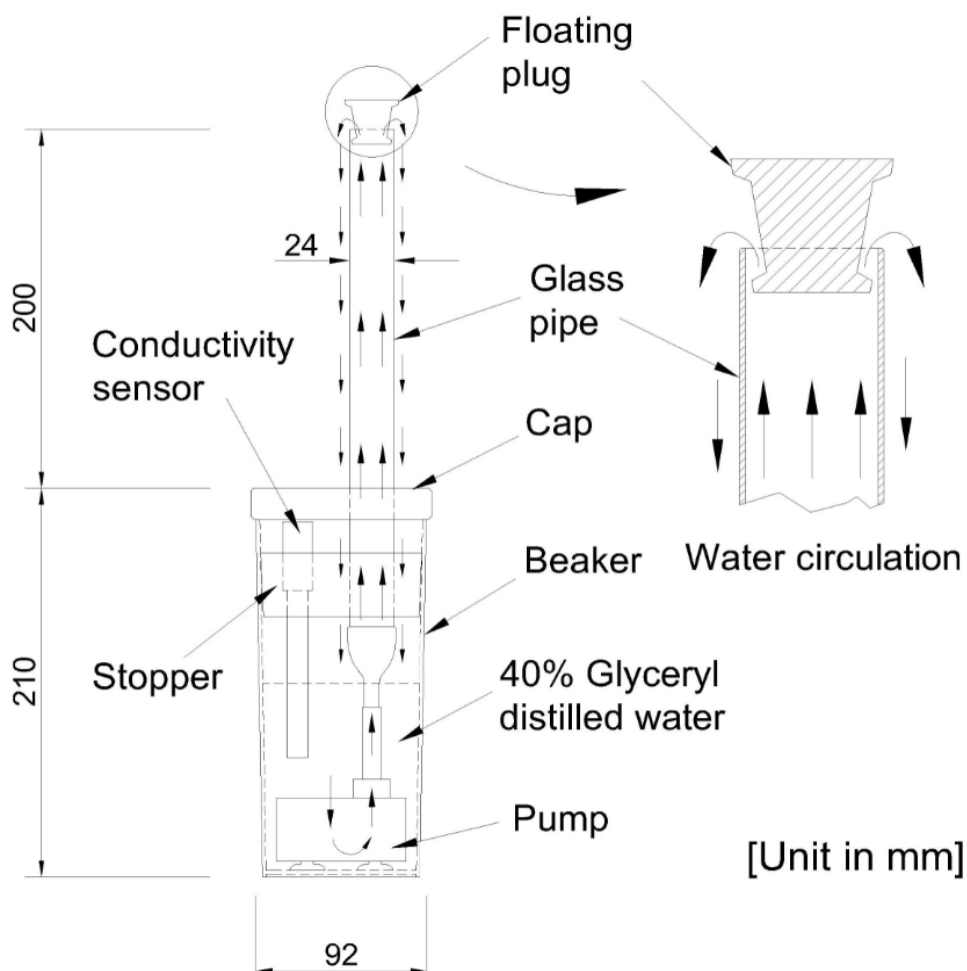


Figure 2 Real-time aerosol chloride measuring device

134

135 **2.2 Calibration of the conductivity sensor**

136 **2.2.1 Conductivity sensor**

137 In this study, a conductivity sensor was applied to measure changes in the conductivity of the solution
138 with a low chloride content. The components of conductivity sensor include a conductivity cell which
139 consists of two electrodes, and a conductivity meter to record the signal from conductivity cell. When the
140 conductivity sensor is immersed into the solution, an alternating voltage signal (V) at 1 kHz is applied to
141 the cell. The response electrical current (I) is measured and conductance (I/V) calculated. The conductivity
142 meter utilises the cell constant, and the conductivity of the sample is finally determined. In this study, the
143 conductivity electrode (model 9382-10D; Horiba Techno Company, Japan) and a conductivity meter

144 (model ES-14; Horiba Techno Company, Japan) was used. The sensor contains a 3-pole cell with a cell
145 constant of 100 m^{-1} .

146 2.2.2 Calibration of conductivity sensor

147 Before the conductivity sensor calibration was conducted, the sensor was conditioned in distilled water
148 for 1 h. During the calibration test, the sensor was simultaneously immersed into solutions of sodium
149 chloride with concentrations ranging from 10^{-6} to 10^{-4} M. This chloride concentration range is based on
150 chloride deposition data of a recent study on long-term aerosol chloride monitoring with weekly sampling
151 frequency in Da Nang city, Vietnam (Pham et al. 2019). All measurements were conducted with a stirred
152 solution in chamber conditions at $18 \text{ }^{\circ}\text{C}$, 32% Rh. The measurement results were recorded when the
153 conductivity of solution becomes constant.

154 The calibration of the conductivity sensor is shown in **Fig. 3**, with a perfect linear relationship between
155 the conductivity and chloride concentration of the test solutions. Therefore, the sensor can be used to
156 measure samples with a low chloride content (10^{-6} to 10^{-4} M).

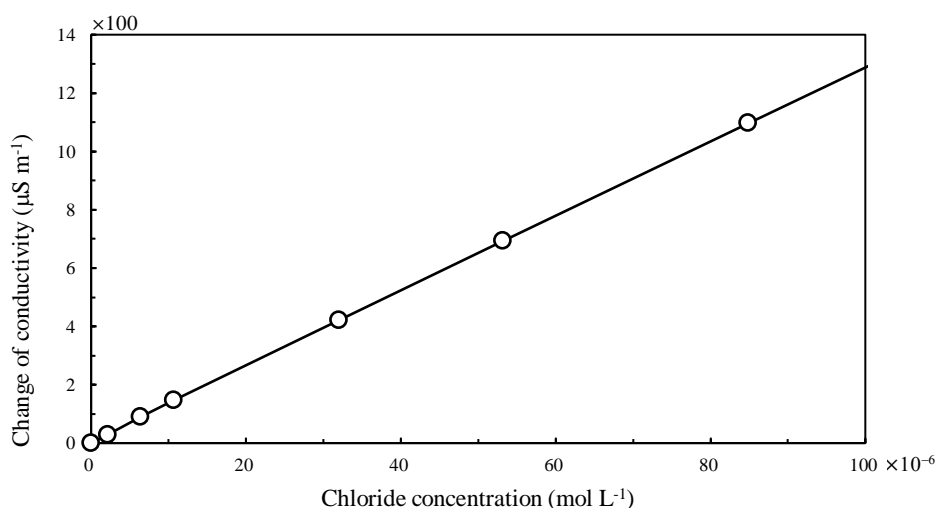


Figure 3 Relationship between conductivity and chloride concentration

157 The conductivity meter used in this study has a high measurement resolution of $0.01 \text{ } \mu\text{S cm}^{-1}$, and thus
158 can detect small changes in chloride ion concentrations, up to $0.1 \times 10^{-6} \text{ mol L}^{-1}$. In our recent research study
159 on long-term monitoring of chloride aerosol (Pham et al. 2019) with a weekly sampling frequency, the
160 absorption spectroscopy method was applied for the chloride analysis. The Absorption spectroscopy device
161 (mode Lamda-9000; Kyoritsu chemical-check Lab., Corp., Japan) and reagent LR-Cl (containing Ag_2SO_4)
162 were used with measurement resolutions of $0.6 \times 10^{-6} \text{ mol L}^{-1}$. Therefore, the conductivity sensor in this
163 study can detect more detailed changes in the chloride ion concentration, compared with those obtained by
164 the absorption spectroscopy method.

165 3. Test

166 **3.1 Laboratory test**

167 The salt aerosol entrainment in an area near the seashore was studied, as salt aerosol generated from the
168 sea is stirred up and entrained inland by wind (Centre, 1996; Spiel and De Leeuw, 1996; Leeuw, 1986). To
169 examine the accuracy and responsiveness of the proposed device, laboratory tests were conducted that
170 simulate salt aerosol entrainment. The tests were composed of three main parts: a salinity aerosol supplier,
171 a wind generator, and the water candle device, as shown in **Fig. 4**.

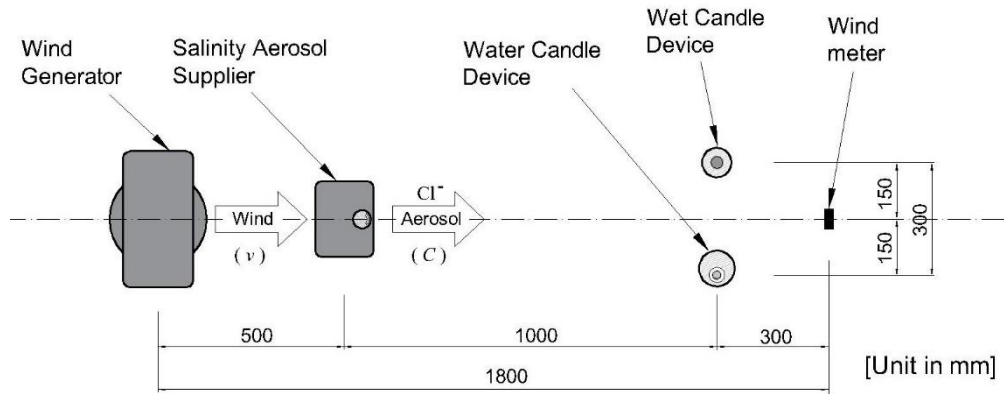


Figure 4 Layout of laboratory test

172 **Figure 4** shows the laboratory test layout. An atomiser (mode 450CH; Levoit Company, USA) with an
173 aerosol output rate of 45 ml h^{-1} was used as the aerosol supplier. An electrical fan (mode AM06DC30WS;
174 Dyson Company, Japan) with stable and adjustable 10-level wind speed output was utilised as the wind
175 generator. The output wind speed ranged from 0.7 to 2.2 m s^{-1} . In every test, a wet candle device was placed
176 next to the water candle device to compare the measured deposition rates by both methods. A wind meter
177 (mode Kestrel 5500-link; Mistral instruments Company, USA) was placed behind the two measuring
178 devices to record the wind speed. Before measuring with the proposed device, a preliminary test was
179 conducted to determine the best positions of the components for which the wind speed was stable. All of
180 the equipment and meters were placed at a height of 1.5 m from the ground. All tests were conducted in a
181 room with constant temperature and a humidity of $18 \text{ }^\circ\text{C}$ and $32\% \text{ Rh}$ without any other airflow. The
182 deposited salinity amount was calculated using the solution conductivity inside the beaker and calibration
183 graphs.

184 **3.1.1 Accuracy test**

185 The device accuracy was tested using certain values of the wind and source salt concentrations. Three
186 different source salt concentrations were used: 3.5% , 17.5% , and 35% . The output wind speed of an
187 electrical fan was adjusted to two levels: levels two ($\sim 1 \text{ m s}^{-1}$) and ten ($\sim 2 \text{ m s}^{-1}$). Each test was conducted

188 for 60 min. The conductivity and wind speed were recorded every 1 min and 5 s, respectively. After each
189 test, the wet candle device was treated and analysed based on the standard (ISO 9225, 2012).

190 3.1.2 Responsiveness test

191 The tests were aimed at evaluating the device responsiveness due to changes in the wind speed for
192 different source salinity concentrations. The tests were conducted with two salinity sources with salt
193 concentrations of 3.5% and 35%. For each salinity source, two tests were performed with ascending wind
194 speeds from wind levels one to ten, and descending wind speeds from levels ten to level one. The ascending
195 and descending steps were 10 mins, thus each test took 100 min.

196 3.2 Field test

197 After the laboratory tests, the device was implemented in a bridge to test the applicability in the field. The
198 device was applied to the monitoring of the Thuan Phuoc Bridge in Da Nang city, Vietnam (**Fig. 5**). Thuan
199 Phuoc Bridge is the longest suspension bridge in Vietnam, with a main span length of 405 m and deck

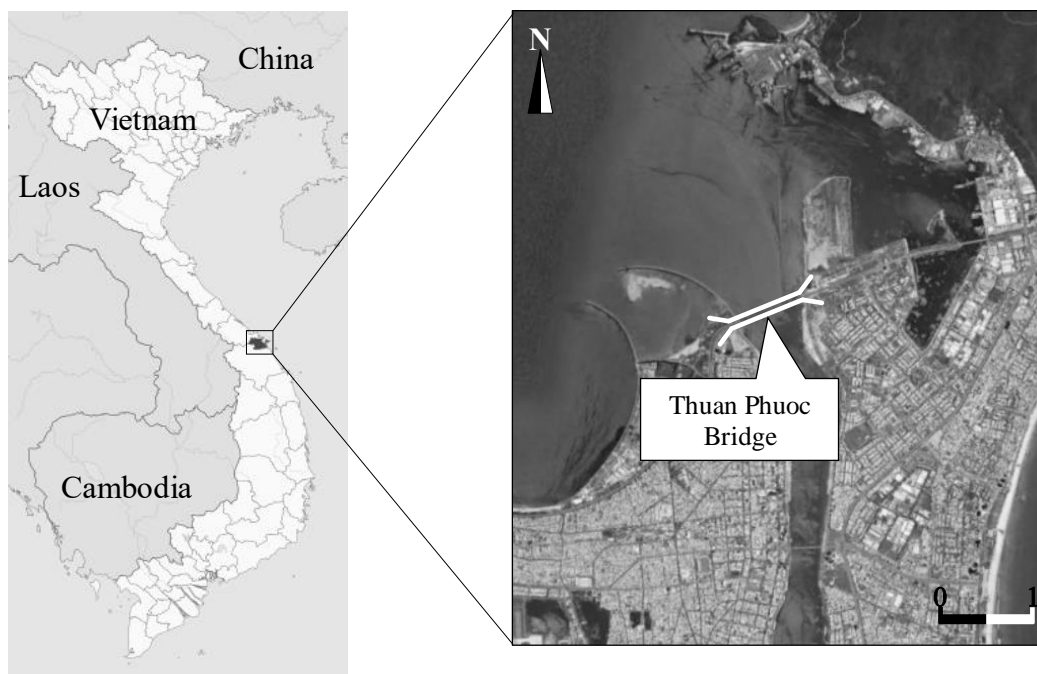


Figure 5 Location of Thuan Phuoc Bridge

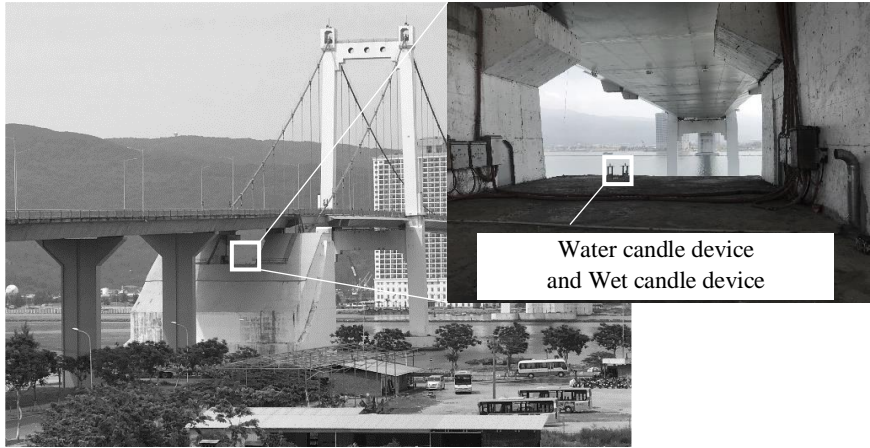


Figure 6 Install location of wet and water candle device

200 elevation of 27 m. The bridge is located far from the industrial zone, at the river mouth of the Han River.
 201 Therefore, the corrosive impact of the marine environment is one of greatest maintenance issues of this
 202 bridge. The measurement system was set on the anchor in front of cable fixing room of Thuan Phuoc Bridge.
 203 This zone is most important part of a suspension bridge. The height of anchor is 27 m from sea level. The
 204 device was placed into a wooden device
 205 holder, as shown in **Fig. 7**. The whole
 206 apparatus was placed on the South
 207 abutment of the bridge at an elevation of
 208 20 m (**Fig. 6**). A wet candle device was
 209 also placed next to the device to compare
 210 the resulting data.

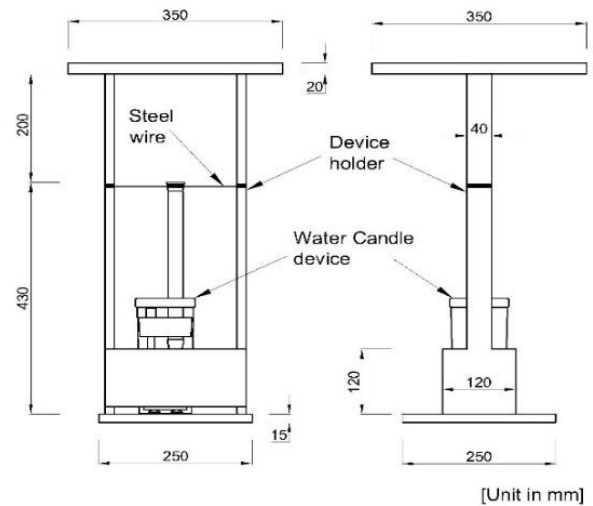


Figure 7 Assembly of water candle

211 In order to keep water film evenly
 212 distributed on the surface of the glass pipe
 213 in all condition of unfavorable weather
 214 events such as strong wind, typhoon, strong gust etc., the horizontal balancing of the supporting frame was
 215 checked and adjusted by a horizontal balance ruler prior to the initial of measurement; the supporting frame
 216 and the floating plug were fixed on concrete ground by steel wires to immobilize the device during strong
 217 wind (**Fig.7**).

218 The measurements were conducted over seven days from May 8, 2018 to May 15, 2018, which is during
 219 the early period of the dry season. The data were recorded at 6:00, 10:00, 13:00, 16:00, 19:00, and 23:00
 220 every day. Due to the considerable evaporation of water, 50 mL of 40% glyceryl- distilled water was poured
 221 into the beaker every day. The chloride amount was calculated by the calibration line of the conductivity

222 sensor, and the volume of the solution was calculated from the solution height. The meteorological data,
 223 such as the temperature, relative humidity, and wind speed, of Da Nang city during the monitoring period,
 224 obtained from a local meteorological station were used for the analysis.

225 4. Results and Discussion

226 4.1 Laboratory Measurements

227 4.1.1. Accuracy test

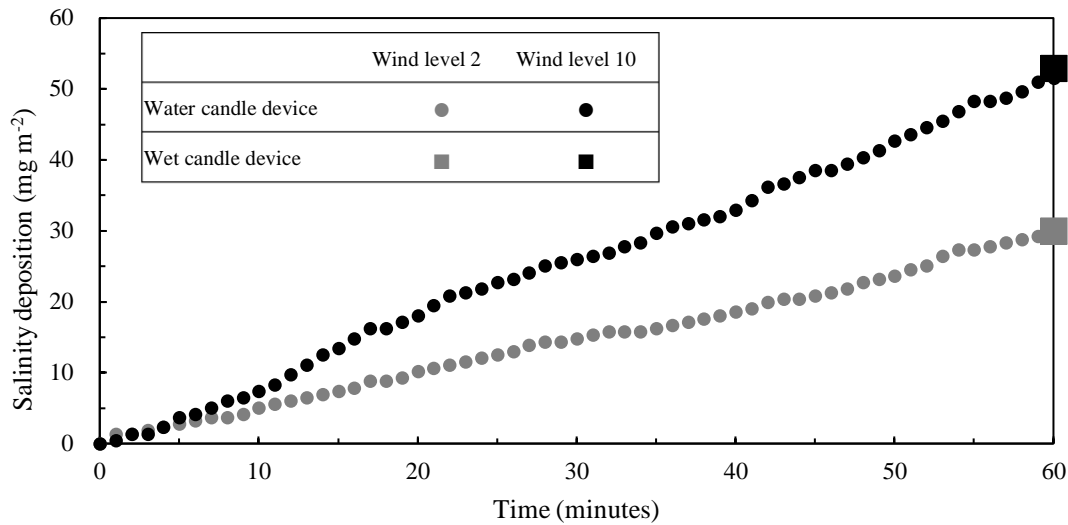


Figure 8 Variation of salinity deposition with time at wind speed levels 2 and 10 (source salt 3.5%)

228 **Figure 8** shows the measured results of the salinity deposition and wind speed of the tests 3.5–2 and 3.5–
 229 10. The salinity deposition is calculated using the ratio of the total deposited salinity and total aerosol
 230 collecting area of the water or wet candles. In **Fig. 8**, there is an almost linear increase in the salinity
 231 deposition in both tests. The wind speeds in the tests 3.5–2 and 3.5–10 were 1.0 and 2.1 m s⁻¹, respectively,
 232 and both had average ± 0.1 m s⁻¹ variations. The salinity depositions measured by the water candle device
 233 in the tests 3.5–2 and 3.5–10 were 30.2 and 51.5 mg m⁻², respectively. The salinity depositions measured
 234 by the wet candle device in the tests 3.5–2 and 3.5–10 were 30.0 and 52.9 mg m⁻², respectively. Therefore
 235 results from the water candle device are in good agreement with the results of the wet candle device.

236 **Table 1** Comparison of measured results of salinity deposition by the wet and water candle devices

Salt concentration	3.5%		17.5%		35.0%
Wind level	2	10	2	10	10
Wet candle device (WeCD) (mg m ⁻²)	30	53	152	253	523
Water candle device (WaCD) (mg m ⁻²)	30	52	147	250	526
Difference rate of WaCD to WeCD (%)	0.7	-2.5	-3.0	-1.1	0.7

237

238 The results using the water and wet candle devices of other tests are listed and compared in **Table 1**. This
 239 table shows the same results for the salinity deposition measured by both devices, with small differences
 240 from 0.7% to 3.0%.

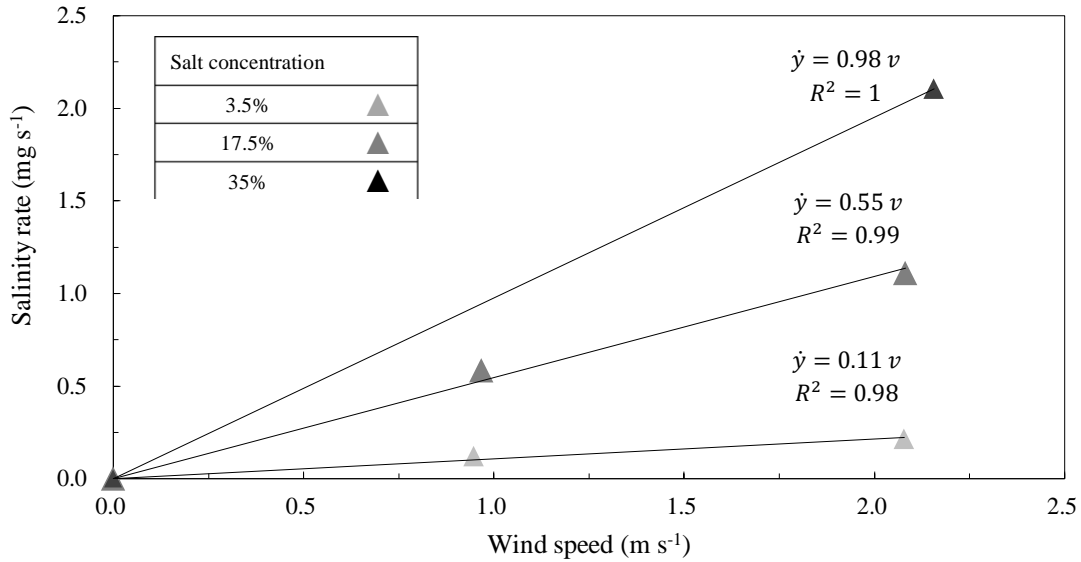


Figure 9 Salinity rate as a function of wind speed

241 **Table 2** shows the salinity rates [salinity deposited per time unit (\dot{y})] for varying average wind speeds
 242 (levels 2 and 10) for five tests. The average level 2 wind speeds were 0.95 and 0.97 m s⁻¹ for salt
 243 concentrations of 3.5% and 17.5%, respectively. The average level 10 wind speeds were 2.08, 2.08, and
 244 2.16 m s⁻¹ in the tests with salt concentrations of 3.5%, 17.5%, and 35% respectively, which were almost
 245 double those of the level 2 wind speeds. The salinity rates (\dot{y}) in the level 10 wind speed tests were almost
 246 double those of the level 2 wind speed test, which were 0.12 mg s⁻¹ and 0.21 mg s⁻¹ (salt 3.5%); and 1.11
 247 and 0.59 mg s⁻¹ (salt 17.5%). **Fig. 9** shows the linear relationship between the salinity rate (α) with the wind
 248 speed (v) for each salt concentration:

249
$$\dot{y} \propto v. \tag{1}$$

250 **Table 2** Salinity rates (\dot{y}) due to wind speed and source salt concentration

Salt concentration (%)	3.5%		17.5%		35.0%	
	Average wind speed (m s ⁻¹)	Salinity rate (g s ⁻¹)	Average wind speed (m s ⁻¹)	Salinity rate (g s ⁻¹)	Average wind speed (m s ⁻¹)	Salinity rate (g s ⁻¹)
2	0.95	0.12	0.97	0.59		
10	2.08	0.21	2.08	1.11	2.16	2.11

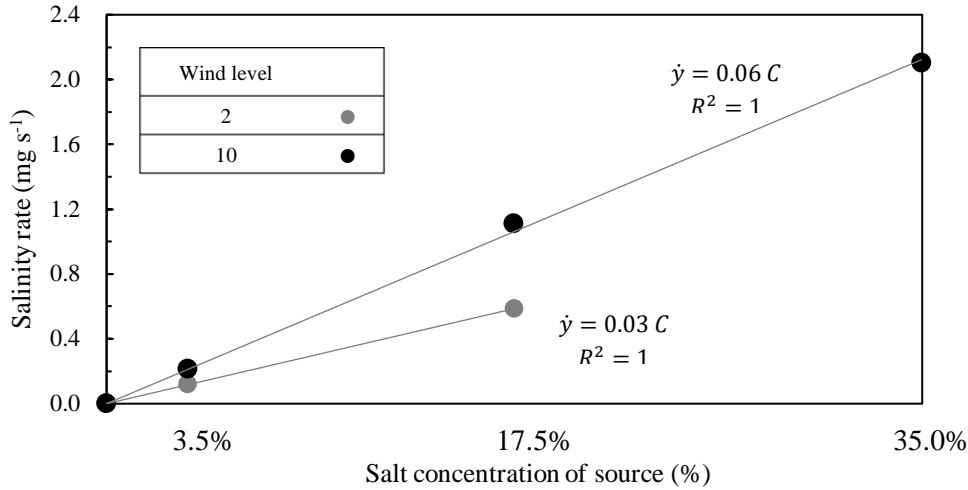


Figure 10 Salinity rate as a function of the source salt concentration

251 For the level 10 wind speed, the measured salinity rate for a salt concentration of 3.5% was 0.21 g s⁻¹,
 252 which was ~5 and ~10 times lower than those of the 17.5% and 35% cases; 1.11 and 2.11 g s⁻¹, respectively.
 253 This tendency is also clearly observed in **Fig. 10**, which shows that the salinity rate is proportional to the
 254 salt concentration source:

255
$$\dot{y} \propto C. \quad (2)$$

256 Using equations (1) and (2), the salinity rate can therefore be expressed as follows:

257
$$\dot{y} = \beta v C \quad (3)$$

258 where y is the total deposited salinity on the measuring device (mg); \dot{y} is the salinity rate (mg s⁻¹); v is the
 259 wind speed (m s⁻¹); C is the salt content of the salinity source (%); and β is the distribution coefficient (mg
 260 m⁻¹).

261 The distribution coefficient (β) was calculated for five tests using equation (3). The calculated results are
 262 shown in **Table 3**. Identified β by each test condition are not so much different each other (0.0029 –
 263 0.0038) and not so much different from the identified β by all test data (0.0032). β can be considered as
 264 a constant and identified value by all tests is used following analysis.

265 **Table 3** Distribution coefficient (β) calculated for five tests using equation (3)

	Salinity concentration of source (%)				
	3.5%	2.08	17.5%	2.08	35.0%
Average wind speed (m s ⁻¹)	0.95	2.08	0.97	2.08	2.16
Distribution coefficient (β) (mg m ⁻¹)	0.0038	0.0029	0.0036	0.0029	0.0029
β identified by all data (mg m ⁻¹)	0.0032				

266 The total deposited salinity for a test time T is obtained by integrating equation (3):

$$267 \quad y = \int_{t=0}^T \dot{y} dt = \beta \int_{t=0}^T C v dt . \quad (4)$$

268 4.1.2 Responsiveness test

269 An analysis of the deposited salinity amount was carried out to compare the results of the responsiveness
 270 tests. As each ascending/descending step was 10 min, and there were ten wind speed levels in total, the
 271 deposited salinity amount, as defined by equation (4), was calculated for each wind speed level with time
 272 intervals of 10 min, as follows:

$$273 \quad y = \sum_{i=1}^{10} y_i = \beta \sum_{i=1}^{10} C v_i \Delta t, \quad (5)$$

274 where i is the time interval order, y_i is the amount of salinity deposited (mg) in the i -th time interval, v_i
 275 is the average wind speed (m s^{-1}) in the i -th time interval, and β is salinity distribution coefficient (mg m^{-1})
 276 (see **Table 3**).

277 **Table 4** Average wind speed and standard deviation for the two cases, ascending and descending, with 10
 278 min intervals (salinity source: 35%) (Unit in m s^{-1})

279	Wind level	1	2	3	4	5	6	7	8	9	10	
	Average	0.8	0.9	1.0	1.2	1.3	1.4	1.6	1.7	1.9	2.0	
280	Ascending	Max	0.8	1.0	1.1	1.3	1.4	1.5	1.7	1.8	2.0	2.1
281		Min	0.7	0.8	1.0	1.1	1.2	1.3	1.5	1.6	1.8	1.9
282	Wind level	10	9	8	7	6	5	4	3	2	1	
	Average	2.1	2.0	1.8	1.7	1.5	1.4	1.3	1.1	1.0	0.8	
283	Descending	Max	2.3	2.1	2.0	1.8	1.6	1.5	1.4	1.2	1.1	0.9
284		Min	2.0	1.9	1.7	1.5	1.4	1.3	1.2	1.0	0.8	0.7

285 **Table 4** shows the average, maximum, and minimum wind speeds for the two cases; ascending and
 286 descending, for 10 min intervals (salinity source: 35%). The scatter of each wind level was small with
 287 variations of ± 0.1 to $\pm 0.2 \text{ m s}^{-1}$.

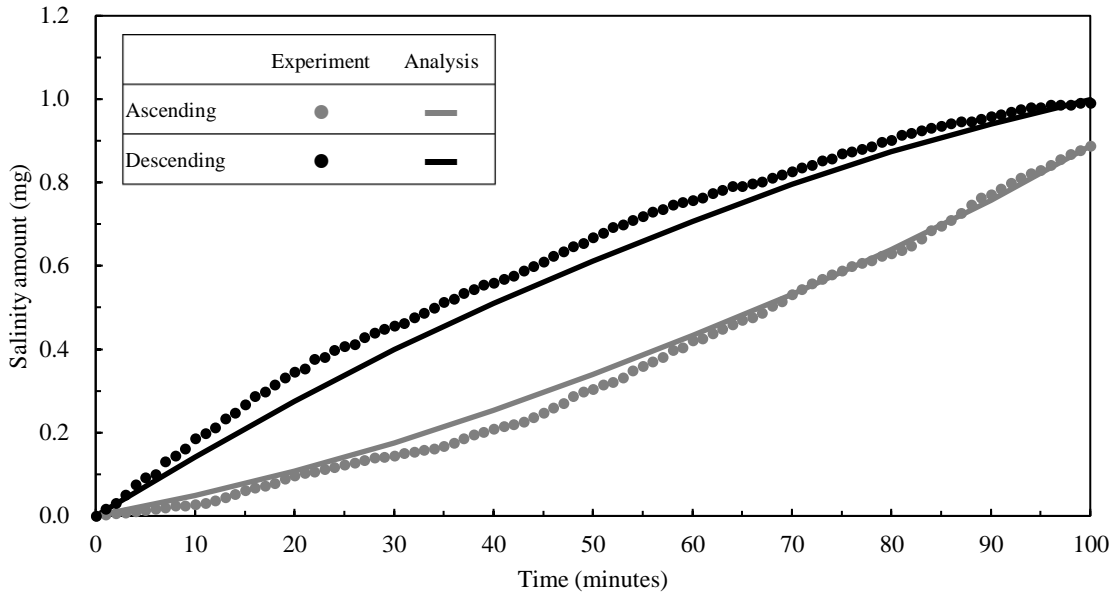


Figure 11 Variation of salinity deposition amount with ascending and descending of wind speed

(Salt source 3.5%)

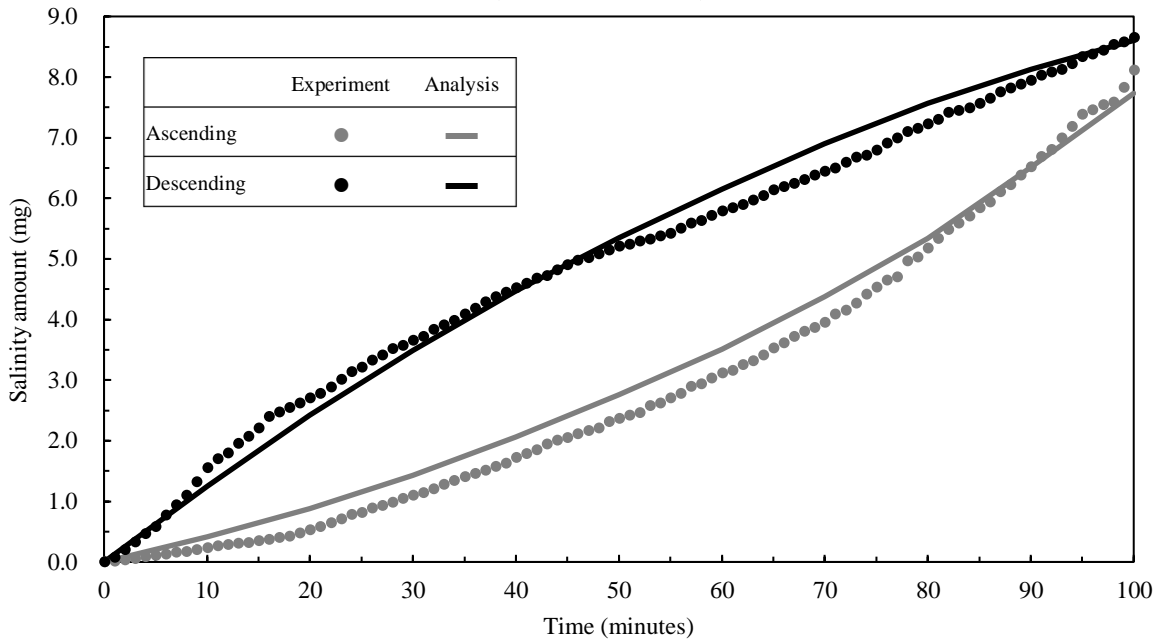


Figure 12 Variation of salinity deposition amount with ascending and descending of wind speed

(Salt source 35%)

288 **Figures 11** and **12** show the analysis and measurement results of the deposited salinity amounts for
 289 ascending and descending wind speeds for the 3.5% and 35% salt concentrations, respectively. For the
 290 3.5% salt concentration, the deposited salinity amounts of the ascending and descending wind speeds were
 291 0.90 and 0.99 mg, corresponding to analytically calculated values 0.89 and 1.00 mg, respectively. For a salt
 292 concentration of 35%, the deposited salinity amounts of increasing and decreasing wind speeds were 8.12
 293 and 8.65 mg, corresponding to analytically calculated values 7.73 and 8.60 mg, respectively. There were

294 small differences between experiment data and analysis data during the measuring period. This may be due
 295 to two main causes. One of them is wind velocity, for analysis it was assumed that the wind speed was
 296 constant during whole one segment of time. But in reality, wind velocity had time lag to reach set velocity
 297 and had fluctuation. Another cause is time lag after aerosol reach to the capturing water film and dilute into
 298 bottle of water then detected by the conductivity sensor. In analysis this is not considered.

299 The plots showed good agreements between the analysis and measurement results. For the ascending wind
 300 speed case, the accumulated salinity followed a polygonal line, with increasing steepness with time.
 301 Conversely, the steepness of the polygonal line was more gradual with time for the descending case. This
 302 is because for increasing/decreasing wind speeds, the salinity rate also increases/decreases, leading to a
 303 different rate of increase for the deposited salinity. Therefore, the device is capable of responding to changes
 304 in the salinity deposition rate due to wind speed variations.

305 **Table 5** Comparison of the deposited salinity amounts of the wet and water candle devices after 100 min
 306 for increasing and decreasing wind speeds (Unit in mg m^{-2}).

	Condition	Water candle (mg m^{-2})	Wet candle (mg m^{-2})	Difference (%)
Salinity concentration 3.5%	Ascending	60	56	6.6
	Descending	67	66	0.2
Salinity concentration 35%	Ascending	555	579	4.1
	Descending	586	563	4.0

307 **Table 5** provides the salinity deposition (mg m^{-2}) measured by the water candle device compared with
 308 that of the wet candle device. There were only small differences in the results of the two devices, with
 309 differences in the rate ranging from 0.2% to 6.6%.

310 In conclusion, the accuracy and responsiveness of the water candle device were confirmed in the
 311 laboratory test. In the accuracy test, the aerosol entrainment condition was fixed and constant, and as a
 312 result, the measured data exhibited a linear increase in the cumulative salinity amount. The results of this
 313 test agreed with those of the wet candle device, with only small differences of 0.2% to 3%. While in the
 314 responsiveness test, the device was tested with a constant salinity source and varying wind speed, and as a
 315 result, the measured data exhibited a polygonal increase corresponding to the wind speed level, providing
 316 a good fit with the calculated results. The difference between the water of the wet candle device in this test
 317 was as small as 6.6%.

318 4.2 Application to monitoring in the field

319 The device worked well without pausing or malfunctioning in the controlled conditions of the laboratory
320 tests. However, in the uncontrolled conditions of the actual environment, the device may malfunction.
321 Moreover, in the field the entrainment of the salinity aerosol is affected by many factors, such as wind,
322 temperature, relative humidity, atmospheric pressure, and rainfall. These factors fluctuate largely and are
323 more complicated than the controlled conditions in laboratory. Therefore, monitoring in the field is
324 necessary to confirm the operation, accuracy, and real-time responsiveness of the water candle device.

325 **Figure 13** shows hourly data of the temperature, relative humidity, atmospheric pressure, and wind speed
326 recorded at a local weather station during the monitoring period. This is typical meteorological data for the
327 early period of the dry season of Da Nang city. There was no rainfall observed in this period. The hourly
328 average temperature, relative humidity, and atmospheric pressure ranged from 24 to 38 °C, 44% to 94%,
329 and 1004 to 1013 hPa, respectively. The temperature and humidity reached peaks near 12:00 AM and
330 dropped to their lowest values near 5:00 AM. The atmospheric pressure peaked near 10:00 AM and 10:00
331 PM every day. The wind speed fluctuated during the day, with the lowest speed in the early morning and
332 highest speed ($\sim 6 \text{ m s}^{-1}$) after noon. These meteorological data showed greater variations in the temperature,
333 relative humidity, and wind speed compared with the laboratory tests.

334 Meteorological factors, such as temperature, humidity, atmospheric pressure, and wind, contribute to the
335 fluctuation of aerosol chloride deposition (Cole, Paterson and Ganther, 2003; Fitzgerald, 199; Gustafsson
336 and Franzén, 2000). While the effect of temperature, relative humidity, and atmospheric pressure is not
337 clear according to the salinity deposition data, the influence of wind speed seems to prevail to other
338 meteorological factors. This agrees with recent researches on the transport of aerosol salinity (Exton et
339 al.1985, Fitzgerald et al.1990). This is because the aerosol salinity is produced from the agitation of sea
340 surface which is due to the wind (Fitzgerald et al.1990, Monahan et al.1971). Also, the wind is major
341 meteorological factor transporting aerosol salinity in land (Morcillo et al.1999; Meira et al.2008). On the
342 other side, other meteorological factors such as relative humidity, rainfall, temperature etc., contribute as
343 additional effect to the motion and concentration of particle (Cole et al.2003).

344 **Figure 14(a)** shows the measured cumulative salinity during the monitoring period. The salinity
345 deposition measured in this period was $\sim 202 \text{ mg m}^{-2}$. This result only differed by 6.8% from that of the wet
346 candle device. **Figure 14(b)** shows the incremental salinity deposition of two continuous recording times.
347 The largest and smallest increments of the salinity deposition measured by the device were ~ 23 and 1 mg
348 m^{-2} , corresponding to 0.5×10^{-6} and $11.5 \times 10^{-6} \text{ M}$, respectively. These values occur in the range of the

349 calibration graph in **Fig. 3**. According to **Fig. 14(b)**, the device detected the deposited salinity in a short
 350 time of a few hours.

351 **Figure 14(c)** shows the average wind speed corresponding to sampling frequency of water candle
 352 device during the monitoring period. The grey bands in **Fig. 14** indicate day light. During this monitoring
 353 period, the sunrise and sunset were near 5:00 and 19:00, respectively. The wind speed tended to increase
 354 after sunrise and decrease after sunset and, reached a peak between 14:00 and 15:00. This is due to the

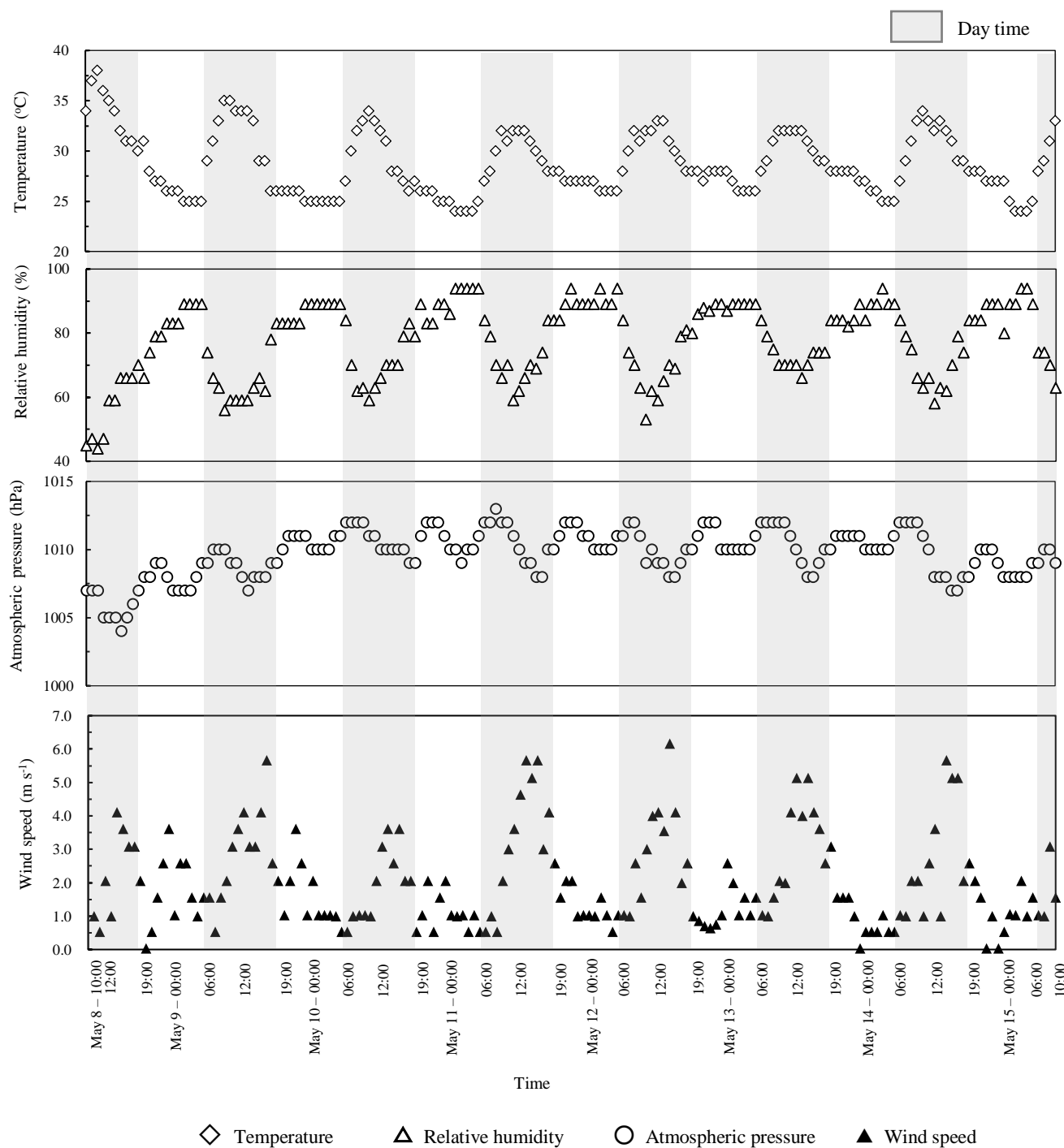


Figure 13 Data of meteorological factors in monitoring period

355 different heating abilities of the sea, earth surface, and air. The measured peak increments of the salinity
 356 deposition were 8, 22, and 10 mg m^{-2} corresponding to wind speeds of 4.1, 5.8, and 5.5 m s^{-1} which are
 357 peak wind speeds in the day. Hence, this demonstrates good functioning of the device for coping with
 358 variations in the wind speed, which cannot be monitored by a wet candle device. Therefore the water candle
 359 device is not only able to measure the salinity deposition with reasonable accuracy compared to the wet

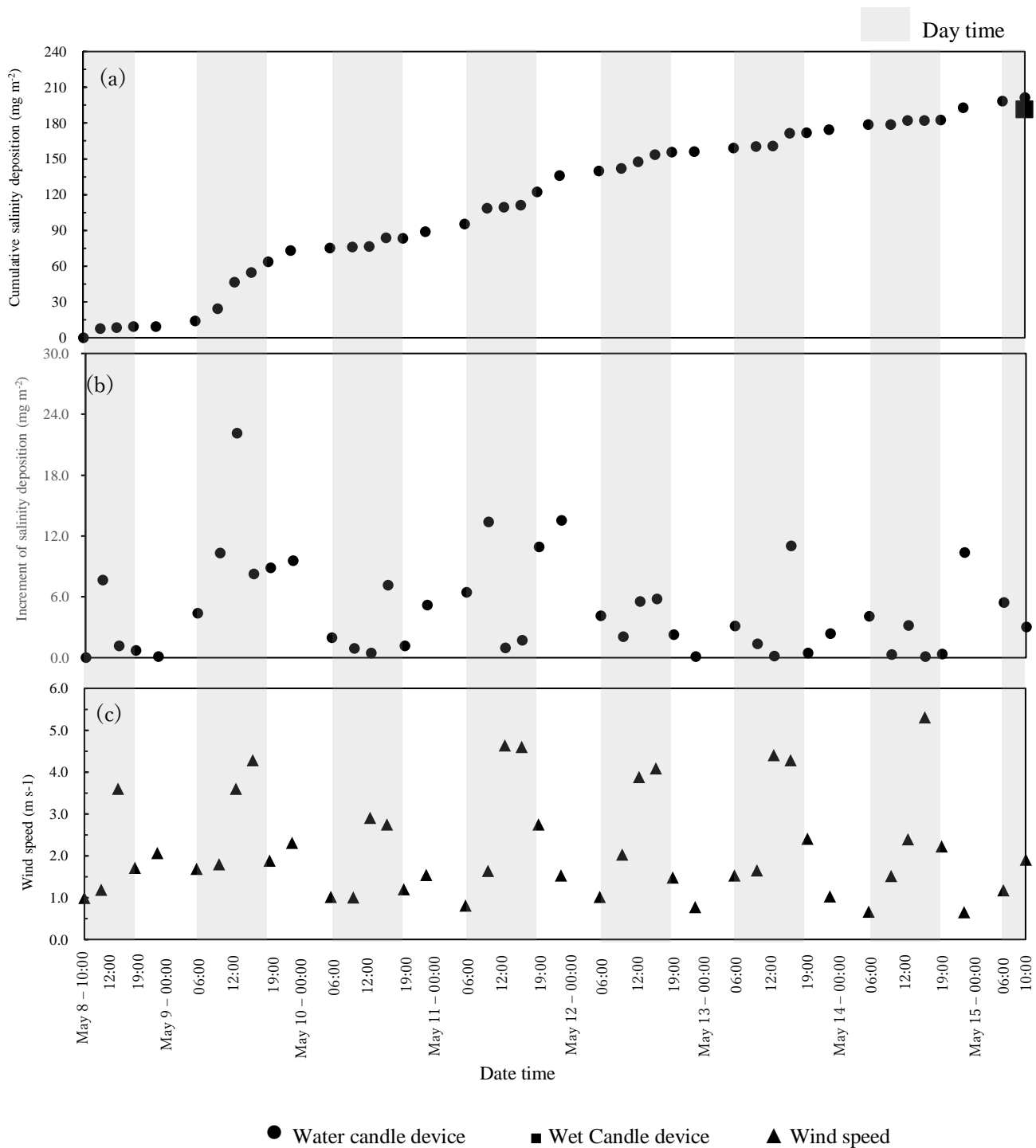


Figure 14 Monitoring results of salinity deposition in Da Nang city and wind speed records

360 candle device, but it is also capable of demonstrating temporal increments in the salinity deposition in real-
361 time.

362 In laboratory test, since the salinity source contains only sodium chloride, there is no other ion dissolved in
363 the solution. In monitoring at the field, other ion may dissolve in the solution and effect the conductivity.
364 However, in this study, since the implemented place of water and wet candle devices were near the shoreline
365 and far from sources of other ions (industrial zone nor forest), the effect of chloride ion on conductivity
366 was predominant and other ion's influence on the conductivity was relatively small. This can be confirmed
367 in comparison between monitored results of water and wet candle devices. However, further study is needed
368 to eliminate the effect of other ions.

369

370 **5. Conclusion**

371 A real-time aerosol chloride measuring device was proposed and tested in the laboratory and in the field.
372 Conditions were set in the laboratory tests to simulate the actual transport of aerosols in area near the
373 seashore to evaluate the accuracy and responsiveness of the device. For monitoring in the field, the device
374 was implemented on the Thuan Phuoc Bridge, Da Nang city for seven days with a short recording frequency.
375 A wet candle device was also placed next to the water candle device to compare the results of both methods.
376 The major conclusions of this study are presented below.

377 1. In the accuracy tests, the measured data exhibited a linear increase in the cumulative salinity amount
378 corresponding to a varied wind speed with a constant salinity source, or varied salinity source with a
379 constant wind speed. The measured result differences between the water and wet candle devices were
380 as small as 0.2% to 3%.

381 2. In the responsiveness test, the measured data exhibited a polygonal increase corresponding to the
382 wind speed level. The analytical calculation of a simple salinity entrainment model was conducted,
383 showing a good agreement with the measured results. Therefore, the water candle device responded
384 well to changing wind speed. The measured result differences between the water and wet candle
385 devices were as small as 6.6%.

386 3. In the field, the device worked well without malfunctioning. The differences in the cumulative
387 salinity deposition measured by the water and wet candle devices were small. The peak increment of
388 the salinity deposition in the day may match the daily peak of wind speed. The results demonstrated
389 the good measuring abilities of the water candle device in the field.

390 **6. Reference**

- 391 Z. Ahmad, Principles of Corrosion Engineering and Corrosion Control. 2006.
- 392 R. W. Revie and H. H. Uhlig, Corrosion and Corrosion Control: An Introduction to Corrosion Science
393 and Engineering: Fourth Edition. 2008.
- 394 F. Corvo, N. Betancourt, and A. Mendoza, “The influence of airborne salinity on the atmospheric
395 corrosion of steel,” *Corrosion science*, vol. 37, no. 12, pp. 1889–1901, 1995.
- 396 H. Silman, “Corrosion and Corrosion Control: An introduction to corrosion science and engineering,”
397 *British corrosion journal*, 1972.
- 398 S. C. Britton, “Metal/Environment Reactions,” *British corrosion journal*, 1976.
- 399 R. T. Foley, “Role of the Chloride Ion in Iron Corrosion,” *Corrosion*, vol. 26, no. 2. pp. 58–70, 1970.
- 400 G. R. Meira, C. Andrade, C. Alonso, I. J. Padaratz, and J. C. Borba, “Modelling sea-salt transport and
401 deposition in marine atmosphere zone - A tool for corrosion studies,” *Corrosion science*, vol. 50, no.
402 9, pp. 2724–2731, 2008.
- 403 G. R. Meira, M. C. Andrade, I. J. Padaratz, M. C. Alonso, and J. C. Borba, “Measurements and modelling
404 of marine salt transportation and deposition in a tropical region in Brazil,” *Atmospheric
405 Environment*, vol. 40, no. 29, pp. 5596–5607, 2006.
- 406 J. W. Fitzgerald, “Marine aerosols: A review,” *Atmospheric Environment. Part A, Gen. Top.*, vol. 25, no.
407 3–4, pp. 533–545, 1991.
- 408 D. E. Spiel and G. De Leeuw, “Formation and production of sea spray aerosol,” *Journal of Aerosol
409 Science*, vol. 27, no. SUPPL.1, pp. S65–S66, 1996.
- 410 M. E. R. Gustafsson and L. G. Franzén, “Inland transport of marine aerosols in southern Sweden,”
411 *Atmospheric Environment*, vol. 34, no. 2, pp. 313–325, 2000.
- 412 G. R. Meira, C. Andrade, C. Alonso, I. J. Padaratz, and J. C. Borba, “Salinity of marine aerosols in a
413 Brazilian coastal area-Influence of wind regime,” *Atmospheric Environment*, vol. 41, no. 38, pp.
414 8431–8441, 2007.
- 415 J. S. Lee and H. Y. Moon, “Salinity distribution of seashore concrete structures in Korea,” *Building and
416 Environment*, vol. 41, no. 10, pp. 1447–1453, 2006.

- 417 F. Delalieux, R. van Grieken, and J. H. Potgieter, “Distribution of atmospheric marine salt depositions
418 over Continental Western Europe,” *Marine Pollution Bulletin.*, vol. 52, no. 6, pp. 606–611, 2006.
- 419 G. R. Meira, W. T. A. Pinto, E. E. P. Lima, and C. Andrade, “Vertical distribution of marine aerosol
420 salinity in a Brazilian coastal area – The influence of wind speed and the impact on chloride
421 accumulation into concrete,” *Construction and Building Materials.*, vol. 135, pp. 287–296, 2017.
- 422 S. Feliu, M. Morcillo, and B. Chico, “Effect of distance from sea on atmospheric corrosion rate,”
423 *Corrosion*, vol. 55, no. 9, pp. 883–891, 1999.
- 424 Anwar Hossain, Khandaker M., Said M. Easa, and Mohamed Lachemi. 2009. “Evaluation of the Effect of
425 Marine Salts on Urban Built Infrastructure.” *Building and Environment* 44 (4): 713–22.
426 <https://doi.org/10.1016/j.buildenv.2008.06.004>.
- 427 Centre, Earth Sciences. 1996. “Dry Deposition and Concentration of Marine.” *Atmospheric Environment*
428 30 (6): 977–89.
- 429 Cole, I. S., D. A. Paterson, and W. D. Ganther. 2003. “Holistic Model for Atmospheric Corrosion Part 1 -
430 Theoretical Framework for Production, Transportation and Deposition of Marine Salts.” *Corrosion*
431 *Engineering Science and Technology*. <https://doi.org/10.1179/147842203767789203>.
- 432 Fitzgerald, James W. 1991. “Marine Aerosols: A Review.” *Atmospheric Environment Part A, General*
433 *Topics* 25 (3–4): 533–45. [https://doi.org/10.1016/0960-1686\(91\)90050-H](https://doi.org/10.1016/0960-1686(91)90050-H).
- 434 Gustafsson, Mats E.R., and Lars G. Franzén. 2000. “Inland Transport of Marine Aerosols in Southern
435 Sweden.” *Atmospheric Environment* 34 (2): 313–25. [https://doi.org/10.1016/S1352-2310\(99\)00198-](https://doi.org/10.1016/S1352-2310(99)00198-3)
436 3.
- 437 ISO (International Organization for Standardization). 2012. “ISO 9225 - Corrosion of Metals and Alloys
438 — Corrosivity of Atmospheres — Measurement of Environmental Parameters Affecting Corrosivity
439 of Atmospheres” 2012.
- 440 JIS Z 2382; 1998. “Determination of Pollution for Evaluation of Corrosivity of Atmospheres.” *Japanese*
441 *Industrial Standard*.
- 442 Lee, Jong Suk, and Han Young Moon. 2006. “Salinity Distribution of Seashore Concrete Structures in
443 Korea.” *Building and Environment* 41 (10): 1447–53.
444 <https://doi.org/10.1016/j.buildenv.2005.05.030>.
- 445 Leeuw, GD. 1986. “Vertical Profiles of Giant Particles Close above the Sea Surface.” *Tellus B*.
446 <http://onlinelibrary.wiley.com/doi/10.1111/j.1600-0889.1986.tb00087.x/abstract>.

- 447 Meira, G. R., C. Andrade, C. Alonso, I. J. Padaratz, and J. C. Borba. 2007. “Salinity of Marine Aerosols
448 in a Brazilian Coastal Area-Influence of Wind Regime.” *Atmospheric Environment* 41 (38): 8431–
449 41. <https://doi.org/10.1016/j.atmosenv.2007.07.004>.
- 450 Meira, G. R., M. C. Andrade, I. J. Padaratz, M. C. Alonso, and J. C. Borba. 2006. “Measurements and
451 Modelling of Marine Salt Transportation and Deposition in a Tropical Region in Brazil.”
452 *Atmospheric Environment* 40 (29): 5596–5607. <https://doi.org/10.1016/j.atmosenv.2006.04.053>.
- 453 Meira, G. R., W. T.A. Pinto, E. E.P. Lima, and C. Andrade. 2017. “Vertical Distribution of Marine
454 Aerosol Salinity in a Brazilian Coastal Area – The Influence of Wind Speed and the Impact on
455 Chloride Accumulation into Concrete.” *Construction and Building Materials* 135: 287–96.
456 <https://doi.org/10.1016/j.conbuildmat.2016.12.181>.
- 457 Morcillo, M., B. Chico, L. Mariaca, and E. Otero. 2000. “Salinity in Marine Atmospheric Corrosion: Its
458 Dependence on the Wind Regime Existing in the Site.” *Corrosion Science*.
459 [https://doi.org/10.1016/S0010-938X\(99\)00048-7](https://doi.org/10.1016/S0010-938X(99)00048-7).
- 460 N. Kazuhiro and D. Yoshiki. 1993. “Nationwide Investigation on Airborne Sea Salt (IV).” *Japan Public*
461 *Works Research Institute*.
- 462 Pham, N.D., Y. Kuriyama, N. Kasai, S. Okazaki, K. Suzuki, and D.T. Nguyen. 2019. “A New Analysis of
463 Wind on Chloride Deposition for Long-Term Aerosol Chloride Deposition Monitoring with Weekly
464 Sampling Frequency.” *Atmospheric Environment* 198.
465 <https://doi.org/10.1016/j.atmosenv.2018.10.033>.
- 466 Spiel, Donald E., and Gerrit De Leeuw. 1996. “Formation and Production of Sea Spray Aerosol.” *Journal*
467 *of Aerosol Science* 27 (SUPPL.1): S65–66. [https://doi.org/10.1016/0021-8502\(96\)00105-X](https://doi.org/10.1016/0021-8502(96)00105-X).

468 **Acknowledgements**

469 This work was supported by a Grant-in-Aid for Scientific Research (B) JSPS KAKENHI Grant No.
470 16H03132, Yokohama National University and The University of Tokyo.

471 **Data Statement**

472 The raw/processed data required to reproduce these findings cannot be shared at this time as the data also
473 forms part of an ongoing study.